

# Multi-Task Anti-Causal Learning for Reconstructing Urban Events from Residents' Reports

Liangkai Zhou

liangkai.zhou@stonybrook.edu  
Stony Brook University  
Stony Brook, New York, United States

Shuqi Zhong

shuqi.zhong@stonybrook.edu  
Stony Brook University  
Stony Brook, New York, United States

Susu Xu

sxu83@jhu.edu  
Johns Hopkins University  
Baltimore, Maryland, United States

Shan Lin

Shan.X.Lin@stonybrook.edu  
Stony Brook University  
Stony Brook, New York, United States

## Abstract

Many real-world machine learning tasks are anti-causal: they require inferring latent causes from observed effects. In practice, we often face multiple related tasks where part of the forward causal mechanism is invariant across tasks, while other components are task-specific. We propose Multi-Task Anti-Causal learning (MTAC), a framework for estimating causes from outcomes and confounders by explicitly exploiting such cross-task invariances. MTAC first performs causal discovery to learn a shared causal graph and then instantiates a structured multi-task structural equation model (SEM) that factorizes the outcome-generation process into (i) a task-invariant mechanism and (ii) task-specific mechanisms via a shared backbone with task-specific heads. Building on the learned forward model, MTAC performs maximum A posteriori (MAP) based inference to reconstruct causes by jointly optimizing latent mechanism variables and cause magnitudes under the learned causal structure. We evaluate MTAC on the application of urban event reconstruction from resident reports, spanning three tasks: parking violations, abandoned properties, and unsanitary conditions. On real-world data collected from Manhattan and the city of Newark, MTAC consistently improves reconstruction accuracy over strong baselines, achieving up to 34.61% MAE reduction and demonstrating the benefit of learning transferable causal mechanisms across tasks.

## Keywords

Causal learning, Urban event reconstruction, Multi-task learning

## 1 Introduction

Many machine learning problems can be interpreted as anti-causal learning problems: estimating the causes given the effects. For example, medical diagnosis [2], image and speech classification [16], and urban event reconstruction [36] are included. In many real-world

problems, the causal mechanism from the cause to the outcome is partially invariant across multiple scenarios. For example, in the problem of urban event reconstruction, urban events, such as illegal parking and unsanitary issues, cause residents' reports through their reporting preferences. The preferences are influenced by the residents' socioeconomic status (SES), such as financial status and educational attainment, with a similar effect across various types of urban events. Air pollution emission source inference is another example [29, 32]. City activities, such as traffic and industry, are causes of various pollutants. The causal effects of these activities on pollutant concentration are similarly influenced by atmospheric patterns such as wind, temperature, and humidity. This shared causal mechanism is also common in clinical diagnosis. Regarding diseases as causes of symptoms, the patients' characteristics, such as age and weight, affect the symptoms similarly across many diseases [19, 25].

However, there are two main challenges to learn the invariant causal mechanism across multiple tasks. First, the causal effects are generated by both task-invariant and task-specific mechanisms. In our problem settings, the causal effects from the confounders to the mechanism variables remain invariant across tasks, whereas the causal effects from the cause to the mechanism variables may vary across tasks. Therefore, it is critical to disentangle and learn the cross-task invariance. Second, our problem also requires anti-causal estimation (i.e., inferring causes from observed outcomes) for individual tasks via the shared mechanism variables.

To address these challenges, we propose a multi-task anti-causal learning framework, *MTAC*. To disentangle the causes from the outcome generation process, we impose a multi-task structural equation model (SEM) that explicitly represents the mechanism variables as latent factors and decomposes their generative process into task-invariant and task-specific components. The invariant causal effect from confounders to the mechanism variables and the task-dependent causal effect from causes to mechanism variables are parameterized by separate neural networks. To address the second challenge, we develop a MAP-based inference algorithm that estimates the causes by jointly optimizing the causes and the shared mechanism variables under the imposed causal structure.

We evaluate the proposed multi-task anti-causal learning framework, *MTAC*, with a real-world application: urban event reconstruction from residents' reports. Urban events refer to localized incidents such as abandoned properties that attract illegal dumping,

Permission to make digital or hard copies of all or part of this work for personal or classroom use is granted without fee provided that copies are not made or distributed for profit or commercial advantage and that copies bear this notice and the full citation on the first page. Copyrights for components of this work owned by others than the author(s) must be honored. Abstracting with credit is permitted. To copy otherwise, or republish, to post on servers or to redistribute to lists, requires prior specific permission and/or a fee. Request permissions from permissions@acm.org.  
*KDD26, Jeju, Korea*

© 2026 Copyright held by the owner/author(s). Publication rights licensed to ACM.  
ACM ISBN 978-1-4503-XXXX-X/2018/06  
<https://doi.org/XXXXXXXX.XXXXXXX>

illegally-parked vehicles that block driveways, sanitary issues like uncollected trash, and crimes in the city. These events collectively drive the quality of life, public safety, and the efficiency of municipal operations. The residents’ reports through digital platforms (e.g., 311 requests [22]) are strong indicators of urban events. These resident-generated reports provide a complementary view of urban conditions and have motivated a growing body of work on estimating and predicting urban events such as crime [4, 33, 40], flooding [1], and parking violations [14]. In practice, residents’ reports of each type of event are observations filtered through human behavior: whether an event is reported depends not only on whether it occurs but also on the likelihood that someone notices it, considers it worth reporting, trusts the reporting channel, and expects a response. Residents’ reporting decisions are shaped by many factors, including neighborhood socioeconomic status (SES), access to technology, language barriers, perceived responsiveness of city agencies, and civic engagement norms [11, 17, 26]. These causal relationships between SES factors and reporting preferences are commonly invariant across types of events. Therefore, jointly learning these causal mechanisms with MTAC could potentially be more robust and benefit each task.

We applied MTAC to three types of urban events: parking violations, abandoned properties, and unsanitary conditions. With the real-world datasets collected from Manhattan and the city of Newark, MTAC significantly outperforms state-of-the-art anticausal learning methods by up to 34.61%.

## 2 Related Works

### 2.1 Multi-Task Learning and Multi-Task Causal Discovery

Multi-task learning (MTL) improves sample efficiency and generalization by sharing representations across related tasks while preserving task-specific components when necessary [6, 30]. This shared-private design principle is particularly relevant when tasks exhibit both common drivers and task-specific dynamics. Separately, a growing line of work studies *multi-task* or *multi-environment* causal discovery, aiming to recover causal graphs by pooling data from multiple related distributions or leveraging invariance across tasks/environments [10, 20, 35]. These methods mainly focus on identifying causal structures (graph recovery) under distribution shifts or heterogeneous datasets. In contrast, our primary goal is to estimate the cause given the outcome and confounders under a multi-task scenario. We formulate a causal discovery problem to capture the most influential confounding factors under assumptions of the causal graph and leverage an anti-causal estimation method to estimate the cause.

### 2.2 Anti-causal Learning and causal prediction

Predicting causes from observed outcomes is fundamentally different from predicting outcomes from causes. In anticausal settings, accurate inference typically requires a generative model that captures how causes produce effects, enabling posterior inference over latent causes given observed effects [27]. Related problems appear in diagnosis, fault localization, and causal abduction, where one seeks likely explanations of observations under a structural causal model [13, 23, 37]. Nevertheless, much of this literature either (i)

does not explicitly leverage the observed outcome information in a structured causal measurement setting, or (ii) relies on strong assumptions such as a observable mediator independent of confounders [18]. Our work targets an anti-causal estimation specific to urban event calibration: reports are outcomes generated from events through a latent reporting-preference mechanism. To address this, we perform maximum a posteriori (MAP) inference of event counts under a learned causal measurement model, effectively “inverting” the forward SEM to reconstruct the event distribution from biased reports.

### 2.3 Urban Event Prediction from Urban Service Data

A large body of work studies urban event prediction, including crime incidents [5, 34, 41], parking violations [15], flooding [1], and other localized urban disorders, from spatiotemporal signals and urban service data such as calls-for-service and 311-style complaints. Common modeling paradigms include spatiotemporal statistical models, point processes, and, more recently, deep learning approaches such as recurrent models and graph-based spatiotemporal networks that incorporate neighborhood context, mobility, and built-environment features [5, 15, 41]. These methods have demonstrated strong predictive performance when the observed event logs are a reliable proxy of true underlying occurrences. However, for many civic issues, the observed “event” records are themselves partially generated by resident reporting behavior or enforcement intensity. Consequently, purely predictive models that treat reported records as ground truth may produce systematically distorted estimates of the event distribution, especially across regions with different socioeconomic status profiles.

## 3 Problem Definition

We aim to estimate the causes from the outcomes and confounders for multiple tasks. Let  $X$  and  $Y$  represent the cause and outcome variables, respectively.  $\mathbf{Z} = \{Z_l \mid l \in \{1, \dots, L\}\}$  represents the confounders.  $X$  affects  $Y$  through  $M$  mechanism variables  $\mathbf{W} = \{W_i \mid i \in \{1, \dots, M\}\}$ .  $\mathbf{W}$  is determined by both the confounders  $\mathbf{Z}$  and the cause  $X$ , i.e.,

$$\mathbf{W} \sim p(\mathbf{W}|\mathbf{Z}, X; \theta^W, \phi^W), \quad (1)$$

where  $\theta^W$  and  $\phi^W$  are parameters of the distribution.  $Y$  is determined by the mechanism variables  $\mathbf{W}$ , i.e.  $Y \sim p(Y|\mathbf{W})$ . Meanwhile, the confounders  $\mathbf{Z}$  also determine the distribution of the cause  $X$ , i.e.,  $X \sim p(X|\mathbf{Z}; \phi^X)$ , where  $\phi^X$  are parameters of its distribution.

We consider  $K$  tasks, where  $X_k$  and  $Y_k$  represent the cause and the outcome in task  $k$ . The causal structure is shown in Figure 1. The distribution of  $\mathbf{W}$  shifts across tasks, and we use the notation  $\mathbf{W}^k$  for task  $k$ . The generation mechanism of  $\mathbf{W}^k$  can be decomposed into a task-agnostic component  $\theta^W$  and task-specific components  $\phi_k^W$ . On one hand, the causal effect of the confounders is shared across tasks, i.e.,  $p(\mathbf{W}^k|\mathbf{Z}; \theta^W)$  holds invariant across tasks with a shared  $\theta^W$ . On the other hand, the causal effect from the cause  $X_k$  varies depending on the task, i.e.,  $p(\mathbf{W}^k|\mathbf{Z}, X_k; \theta^W, \phi_k^W)$  shifts across task  $k$  with varying  $\phi_k^W$ . This hybrid task-agnostic and task-specific causal mechanism holds for many real-world problems, as discussed in the introduction. For each task  $k$ , we aim to estimate the

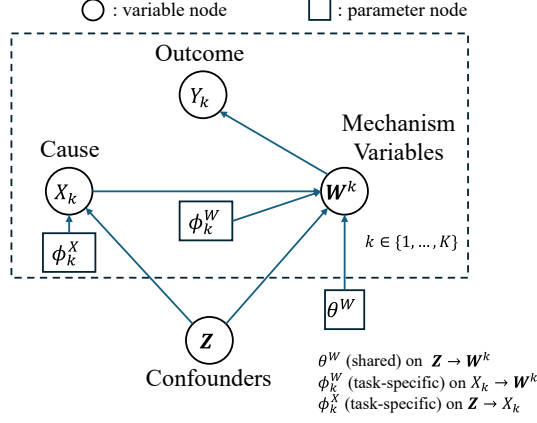


**Figure 1: Multi-task causal graph with shared causal mechanism.**

distribution of the cause  $X_k$  given the outcome  $Y_k$  and confounders  $Z$ , i.e.,  $p(X_k|Y_k, Z)$ .

#### 4 Multi-task Structural Causal Model

To estimate  $X_k$  from  $Y_k$  for task  $k$ , it is crucial to model the generation process of  $Y_k$ , which is a hybrid of task-invariant and task-specific causal mechanisms. Given the heterogeneous datasets for each task, joint training across tasks provides an opportunity to learn a more generalizable and accurate task-invariant causal mechanism. Therefore, we propose MTAC to model the generative mechanism of  $Y$  across multiple tasks. Figure 2 illustrates the framework of MTAC. As shown on the left side of Figure 2, a multi-task SEM is constructed to represent the causal relationship. The causal structure is constructed according to Section 3. The cause and outcome in each task are modeled as separate variables. The mechanism variables and confounders are modeled as shared variables across tasks. The conditional distribution of each variable is modeled with a neural network module, represented as white nodes. Drawing samples from distributions is represented with gray nodes. As shown in the orange box in Figure 2, for the mechanism variable  $W_1$ , we explicitly use separate neural networks to capture the task-agnostic causal effects from  $Z$  and the task-specific causal effects from  $X_k$ . To address the anti-causal estimation based on the learned SEM, we employ a MAP-based inference algorithm to estimate the cause  $X_k$ , as shown on the right side of Figure 2.

##### 4.1 Multi-task Structural Causal Model

Let  $\mathbf{n}$  represent the vector of all variables, which consists of  $X_k$ ,  $Y_k$ ,  $Z$ , and  $W^k$ . Notably, in our problem, the mechanism variables  $W^k$  are difficult to observe directly and are modeled as latent variables. For notation simplicity, we also use variable set notations to represent indices. Let  $I_X = \{i : \mathbf{n}_i \in X\}$  and  $\mathbf{n}_X$  denote the elements of  $\mathbf{n}$  with indices in  $I_X$ . The causal graph is represented with an adjacency matrix  $A \in \{0, 1\}^{|\mathbf{n}| \times |\mathbf{n}|}$ , which can be learned by causal discovery [1]. Specifically, when  $\mathbf{n}_i$  is a cause of  $\mathbf{n}_j$ , we have  $A_{i,j} = 1$ . And  $A_{i,j} = 0$  otherwise. Let  $\text{pa}_i$  represent the causes of the  $i$ -th variable, and we have  $\text{pa}_i = A_{i,:} \odot \mathbf{n}$ . A structural equation model for the  $i$ -th variable

$\mathbf{n}_i$  is constructed as

$$p(\mathbf{n}_i|\text{pa}_i) \sim \mathcal{N}(f_\theta^\mu(A_{i,:} \odot \mathbf{n}), f_\theta^\sigma(A_{i,:} \odot \mathbf{n})). \quad (2)$$

$f_\theta^\mu(\cdot)$  and  $f_\theta^\sigma(\cdot)$  fit the mean and variance of  $p(\mathbf{n}_i|\text{pa}_i)$  respectively.  $f_\theta^\mu(\cdot)$  and  $f_\theta^\sigma(\cdot)$  are fitted using neural networks with parameter  $\theta$ . For variables  $X$  and  $Y$ ,  $f_\theta^\mu(\cdot)$  and  $f_\theta^\sigma(\cdot)$  are modeled with multi-layer perceptron (MLP) networks. Particularly, to explicitly model the task-agnostic and task-specific effects on the mechanism variables  $W$ , the SEMs in Eq. 2,  $f_\theta^\mu(\cdot)$  and  $f_\theta^\sigma(\cdot)$ , are modeled with a multi-task mechanism module. Details are discussed in Section 4.2.

We construct the causal graph  $A$  with prior knowledge, as illustrated in Figure 1. For task  $k$ , the outcome  $Y_k$  is generated through the mechanism variables  $W^k$ . The  $W^k$  is generated with both the confounders  $Z$  and the cause  $X_k$ . The adjacency matrix  $A$  should identify the significant confounders from data, while satisfying the causal relationship in Figure 1. As such, the adjacency matrix is partitioned into two parts as:

$$A = A^{\text{learn}} \cdot M + A^{\text{fix}}, \quad (3)$$

where  $A^{\text{learn}}$ ,  $A^{\text{fix}} \in \{0, 1\}^{|\mathbf{n}| \times |\mathbf{n}|}$  represent a learnable component and a fixed component that represents prior knowledge, respectively.  $M \in \{0, 1\}^{|\mathbf{n}| \times |\mathbf{n}|}$  is a mask matrix, where  $M_{i,j} = 1$  indicates that  $A_{i,j}$  is learnable. To ensure that the learned  $A$  satisfies the pre-defined causal structure in Figure 1, we force  $A^{\text{fix}}$  as

$$A_{W,Z}^{\text{fix}} = A_{X,Z}^{\text{fix}} = A_{Y,:}^{\text{fix}} = A_{W,X}^{\text{fix}} = 0, \quad (4)$$

so that the following edges are forbidden: 1)  $W$  to  $Z$ ; 2)  $X$  to  $Z$ ; 3)  $Y$  to other variables; and 4)  $W$  to  $X$ . The learnable component  $A^{\text{learn}}$  identifies the parent variables of the cause  $X_k$  and the mechanism variables  $W$ . Injecting such prior knowledge improves training efficiency by trimming the parameter space and avoiding potential spurious causal relationships.

##### 4.2 Multi-task Mechanism Module

The mechanism variables are generated under both task-specific effects and task-shared effects. For task  $k$ , the task-specific effects arise from the cause  $X_k$ , while the task-shared effects arise from the confounders  $Z$ . For example, in the urban event reconstruction problem, residents' reporting preferences are affected by both the occurrence of urban events and the SES of residents. The causal effect of urban events on reporting preferences varies across event types, reflecting the varying propensity of residents to report different categories of incidents [12]. Meanwhile, the causal effect of residents' SES on reporting preferences is invariant across event types. For example, highly educated residents tend to have greater confidence in the effectiveness of formal complaints; consequently, they are more inclined to report problems irrespective of the specific event category [11].

To model both causal effects, we construct a multi-task SEM for each mechanism variable. The model structure is illustrated in Figure 3. For a mechanism variable  $W_i$ , a task-shared backbone with parameter  $\theta_i^W$  transforms the parental confounders  $\text{pa}_Z(W_i)$  into an embedding that represents the task-shared causal effect prior  $p(W_i|\text{pa}_Z(W_i))$ . Then, for task  $k$ , the embedding is concatenated with  $X_k$  and fed to task-specific heads  $\phi_{i,k}^W$  to generate  $W_i^k$ . This structure captures both the shared reporting preference and the

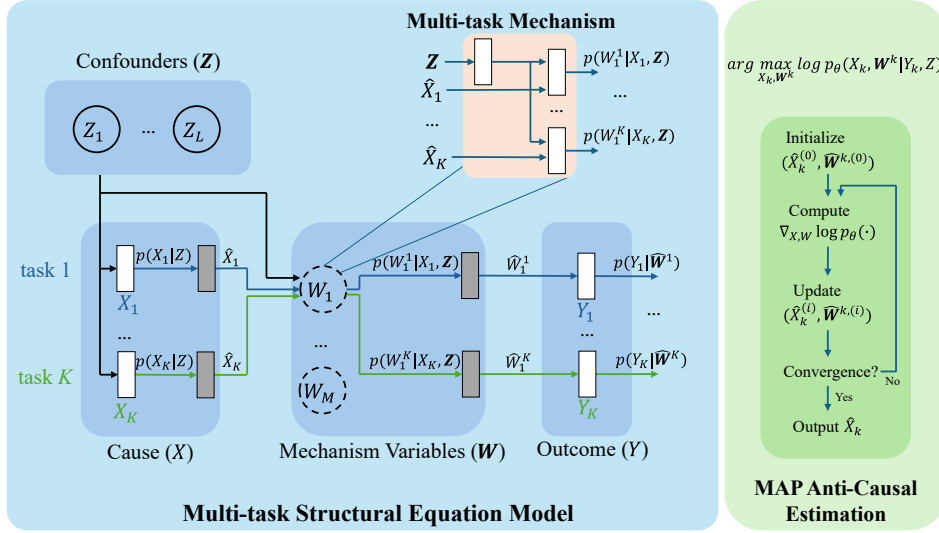


**Figure 2: MTAC Framework.** The white nodes represents parameterized deterministic neural networks, gray nodes represents drawing samples from the respective distribution.

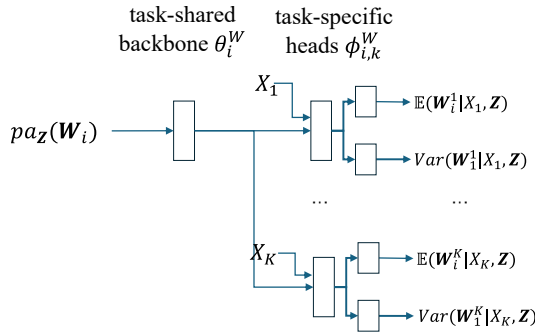


**Figure 3: Multi-task SEM for mechanism variable  $W_i$ .** Each block represents an neural network module. task-specific reporting mechanism as

$$\mathbf{W}_i^k \sim p(\mathbf{W}_i^k | \text{pa}_Z(\mathbf{W}_i^k), X_k; \theta_i^W, \phi_{i,k}^W). \quad (5)$$

Notably,  $\theta_i^W$  is shared across tasks. As a result, the causal effect  $p(\mathbf{W}_i^k | \text{pa}_Z(\mathbf{W}_i^k); \theta_i^W)$  is captured explicitly by the task-shared backbone.

### 4.3 MAP Anti-Causal Estimation

The proposed forward causal model enables the estimation of the cause  $X_k$  of all tasks from its parental variables directly. However, as discussed in Section 4.1, such naive estimation does not leverage information of the outcome  $Y_k$ . Therefore, we develop a MAP-based inference algorithm to estimate the cause leveraging the outcome information. For task  $k$ , the value of  $X_k$  can be estimated with its posterior

$$(\hat{X}_k, \hat{\mathbf{W}}^k) = \max_{X_k, \mathbf{W}^k} p_\theta(X_k, \mathbf{W}^k | Y_k, \mathbf{Z}), \quad (6)$$

where  $\theta$  represents the parameter of the SEM. Since  $p_\theta(X_k, \mathbf{W}^k | Y_k, \mathbf{Z}) \propto p_\theta(X_k, Y_k, \mathbf{W}^k, \mathbf{Z})$ , it is equivalent to solve

$$(\hat{X}_k, \hat{\mathbf{W}}^k) = \arg \max_{X_k, \mathbf{W}^k} \log p_\theta(X_k, Y_k, \mathbf{W}^k, \mathbf{Z}). \quad (7)$$

Notably, in equation (7), we also optimize over the mechanism variables  $\mathbf{W}^k$  because they are latent and uncertain. Updating them makes the inference more stable.  $p_\theta(X_k, Y_k, \mathbf{W}^k, \mathbf{Z})$  can be directly estimated with the forward causal model through the causal order as

$$\log p_\theta(\mathbf{n}) = \sum_i \log p_\theta(\mathbf{n}_i | \text{pa}_i). \quad (8)$$

Thus, equation (7) can be solved with gradient-based optimizers since the SEM is constructed using differentiable neural networks. We first initialize  $X_k$  as  $p_\theta(X_k | \text{pa}(X_k))$  by inferring the causal model. Similarly, mechanism variables  $\mathbf{W}^k$  are initialized by inferring the SEM as well. Then,  $X_k$  and  $\mathbf{W}^k$  are optimized by solving equation (7) using gradient descent methods, while  $\theta$  is frozen. The procedure is illustrated in Algorithm 1.

This event inference algorithm bridges the coupled multi-task anti-causal estimation and the shared causal mechanism. The mechanism variables  $\mathbf{W}^k$  are generated jointly by the  $X_k$  and  $\mathbf{Z}$ . As a result, the same  $Y_k$  can be explained by either (1) a high causal effect from  $X_k$  with a low effect from  $\mathbf{Z}$ , or (2) a lower effect from  $X_k$  with a higher effect of  $\mathbf{Z}$ . Taking an example of the urban event reconstruction problem, the same amount of reports can indicate a high amount of urban events with low reporting willingness, or a low amount of events with high reporting willingness. The proposed multi-task causal model supplies a transferable prior on latent mechanism variables, and the MAP inference algorithm leverages it to disentangle reporting bias from true event frequency. Equation (6) can be decomposed to

$$\begin{aligned} \arg \max_{X_k, \mathbf{W}^k} \log p_\theta(Y_k | \mathbf{W}^k) + \log p_\theta(\mathbf{W}^k | X_k, \mathbf{Z}) \\ + \log p_\theta(X_k | \mathbf{Z}). \end{aligned} \quad (9)$$

The first term represents the reporting model, which forces the inferred  $\mathbf{W}^k$  to explain the observed outcome  $Y_k$ . The second term represents the shared multi-task prior, which regularizes  $\mathbf{W}^k$  toward the value learned jointly across multiple tasks. The third term represents the task-specific cause prior, which prevents degenerate

**Algorithm 1** MAP-based event inference

---

**Input:** Observation of outcome  $Y_k$  and confounders  $Z$   
**Output:** Estimation of cause  $X_k$   
Initialize  $X_k = \max p_\theta(X_k|Z)$ .  
Initialize  $\mathbf{W} = \max p_\theta(\mathbf{W}|X_k, Z)$ .  
**repeat**  
  Compute joint log probability density  $\log p_\theta(\mathbf{n}) = \sum_i \log p_\theta(\mathbf{n}_i|pa_i)$  with SEM  $\theta$ .  
  Update  $X_k$  and  $\mathbf{W}$  to minimize  $-\log p_\theta(\mathbf{n})$  with gradient descent method.  
**until** convergence

---

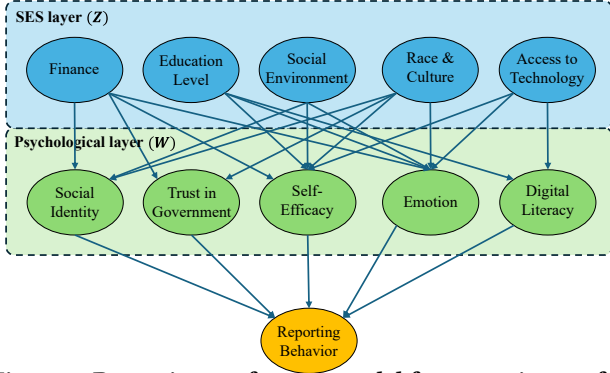


**Figure 4: Reporting preference model for reporting preference.** The SES of residents affect their reporting preference through a set of psychological paths. event estimates that fit  $Y_k$  only by inflating  $X_k$ . As such, solving equation (6) balances the task-specific and task-shared causal effects.

#### 4.4 Training

The learning parameters of MTAC include the network parameters  $\theta$  and the adjacency matrix  $A$ . The loss function consists of two parts:

$$\mathcal{L} = \mathcal{L}_{\text{nll}} + w \cdot \mathcal{L}_{\text{acyc}}, \quad (10)$$

where  $w$  represents a tunable weight.  $\mathcal{L}_{\text{nll}}$  represents the negative log likelihood loss, and  $\mathcal{L}_{\text{acyc}}$  represents an acyclic constraint for  $A$ . For variables  $\mathbf{n}_i$ , we compute the negative likelihood loss as

$$\mathcal{L}_{\text{nll}}^i = -\log p_\theta(\hat{\mathbf{n}}_i|pa_i), \quad (11)$$

which represents the probability of  $\mathbf{n}_i$  conditional on its parental variables and can be computed directly from the SEM. The overall negative log likelihood loss is  $\mathcal{L}_{\text{nll}} = \sum_i \mathcal{L}_{\text{nll}}^i$ . Inspired by [39], to ensure  $A$  depicts a valid directed acyclic graph (DAG), we construct the acyclic constraint as

$$\mathcal{L}_{\text{acyc}} = \text{tr}(\exp(A \odot A)) - |\mathbf{n}|, \quad (12)$$

where  $\text{tr}(\cdot)$  represents the trace function. We relax  $A$  to the continuous domain to enable gradients. Therefore, a threshold  $t_A$  is applied to determine the existence of a causal relationship.

### 5 A Case Study: Urban Event Reconstruction

Urban event reconstruction is an application where multi-task anti-causal learning being effective. Residents submit reports upon observing various urban events, such as parking violations, abandoned

properties, and unsanitary sites. This procedure can be understood as a causal generation, where urban events cause residents' reports through a causal mechanism representing their reporting preferences, which are influenced by the residents' socioeconomic status [11]. Thus, the causal model for urban report generation is modeled as follows: 1) cause ( $X$ ): number of urban events; 2) outcome ( $Y$ ): number of resident reports; 3) confounders ( $Z$ ): residents' SES; 4) mechanism variables ( $W$ ): residents' reporting preference.

The residents' reporting preference is widely studied in social research [11, 24]. The SES factors affecting residents' reporting preferences can be categorized into 5 categories: 1) financial, 2) educational attainment, 3) race and culture, 4) access to technology, and 5) social environment. For example, people with higher educational attainment often trust more that their complaints will be addressed [9]. Social studies [17, 26] have investigated how residents' SES affects their reporting behavior through psychological pathways. We summarize 5 core psychological factors:

- **Social Identity:** A strong sense of community identity increases individuals' willingness to engage in public participation [17]
- **Trust in Government:** Trust in public institutions significantly correlates with the decision to submit complaints [17]
- **Self-Efficacy:** People who feel capable of changing their environment are more likely to participate [26]
- **Emotion:** Positive emotional states facilitate participation, while frustration or apathy may suppress action [17]
- **Digital Literacy:** Individuals without adequate internet access or devices are systematically excluded from participating in online civic activities [26].

As a result, a reporting preference model is defined as shown in Figure 4. Notably, these psychological pathways are independent of the urban event type. Therefore, learning a unified reporting preference model across multiple tasks is more generalizable and may benefit each task. The causal effect of urban event occurrence is task-specific, reflecting the heterogeneous reporting propensities of residents toward different categories of urban incidents [12]. As such, the multi-task causal mechanism design in MTAC would explicitly capture both the task-shared and task-specific causal effects of residents' reporting behavior.

## 6 Evaluation

### 6.1 Datasets

We evaluate our design for the application of urban event reconstruction. Three types of urban events are considered: 1) parking violations, 2) abandoned properties, and 3) unsanitary conditions. For abandoned properties, we collect data from the City of Newark. The reports are collected from the SeeClick platform [28]. This is an online platform where residents can submit complaints about various urban issues. We collect the labels of abandoned properties from the historical records of the City of Newark, which track and monitor abandoned properties. We use this information to count the number of abandoned properties during each time period. We collect the data from 2019 to 2023 in Newark.

We collect data on parking violations and unsanitary issues from Manhattan in 2023. The residents' reports are collected from the NYC311 platform. The ground-truth of parking violations is collected from the database of parking violation tickets provided

Model	Parking Violation		Abandoned Property		Unsanitary Condition	
	MAE	MSE	MAE	MSE	MAE	MSE
MTAC	<b>0.2901</b>	<b>0.1634</b>	<b>0.4280</b>	<b>0.1901</b>	<b>0.3828</b>	<b>0.2496</b>
CEVAE	0.3235	0.1925	0.4867	0.2607	0.4091	0.2884
TEDVAE	0.4315	0.2636	0.4932	0.2583	0.4188	0.2700
BSM-UR	0.4437	0.2976	0.5438	0.3175	0.3982	0.3026
PLE	0.3337	0.2174	0.4533	0.2351	0.4101	0.2697

**Table 1: MAE and MSE estimation for MTAC and baselines across three tasks.**

Category	Factors
Finance	mean income, unemployment rate, mortgage ratio, poverty rate, housing cost
Education Attainment	% less than high school, % high school, % bachelor or higher
Race & Culture	% Hispanic, % white, % black, % Asian
Access to Technology	% has computer, % has smartphone, % has internet
Social Environment	population, % multifamily, % owner occupied, % renter occupied, median year built, % room occupation $\geq 0.5$ , mobility rate

**Table 2: An overview of the socioeconomic status factors.**

by the department of finance [8]. The ground-truth of unsanitary conditions is collected from the hearing records of the city’s administrative law court [7].

The cities are partitioned based on census tracts, and we collect the residents’ socioeconomic status in each region from the census bureau database [31]. As a result, the city of Newark is partitioned into 88 regions, and Manhattan is partitioned into 322 regions. We count the frequency of urban events and reports every month. The socioeconomic status factors include 5 categories, as shown in Table 2. There are 22 factors collected, and the details of each factor can be found in [31].

## 6.2 Evaluation Setting

We compare the performance of MTAC with several state-of-the-art methods:

**BSM-UR** [1]: A Bayesian spatial latent-variable model that recovers the underlying true event incidence from biased reports. BSM-UR does not model the causal mechanism of generating resident reports. It only considers a single type of event.

**PLE** [30]: A multi-task learning architecture that stacks customized gate-control layers to progressively extract shared and task-specific features via mixtures of shared/task experts. PLE does not model the causal relationship between inputs and outputs.

**CEVAE** [13]: A deep latent-variable causal model that uses a variational autoencoder to account for hidden confounding and enables counterfactual/causal-effect inference (and posterior inference over latent causes) from observational data. CEVAE is designed for causes of binary values. To adapt to causes of continuous values, we replace the networks  $q(y|t=1, x)$  and  $q(y|t=0, x)$  with a network  $q(y|t, x)$  that takes the cause  $t$  as input. To estimate the cause, the  $p(t|z)$  network in the decoder is inferred.

**TEDVAE** [38]: A variational latent-factor causal model that infers hidden factors from observed covariates and disentangles them into instrumental, confounding, and risk components. To evaluate TEDVAE, the SES variables are categorized into these three groups based on the causal discovery result. To adapt to the causes of

continuous values, TEDVAE is modified in the same way as CEVAE. We infer the auxiliary classifier  $q_{wr}(t|z_t, z_c)$  for cause estimation. TEDVAE does not employ multi-task learning.

The multi-task SEM is implemented according to Figure 1. Each neural network block (the white nodes) is implemented using an MLP with a hidden dimension of 64. For the mechanism variables, their generation is fitted with the module in Figure 3, where each neural network block is also implemented using an MLP with a hidden dimension of 64. As discussed in Section 5, we set the number of mechanism variables as  $|W| = 5$  to represent the psychological pathways that affect reporting behavior. 80% of the data is used for training and validation, while the other 20% is used for evaluation. Z-score normalization is applied. Since BSM-UR, CEVAE, and TEDVAE does not employ multi-task learning, they are trained and evaluated on each task separately.

The event distribution prediction error is evaluated as the difference between the inferred value of the urban event count and the ground-truth. We measure the prediction error using MAE and MSE. To validate the contribution of the task-agnostic causal mechanism, we also compare the prediction error when trained separately on each task and when jointly trained across three tasks. Moreover, we learn MTAC on two tasks and transfer the task-shared backbone to the other task to validate that the causal effects from the SES factors are task-agnostic. Ablation studies are conducted to illustrate the contribution of each component in MTAC. We also present the causal discovery result by MTAC, which identifies the causing factors of urban events that are consistent with social studies.

## 6.3 Prediction Error

Table 1 presents MTAC’s prediction error against other baselines. We can see that MTAC outperforms all baselines. CEVAE, TEDVAE, and BSM-UR do not consider the shared causal generative mechanism and are trained for each task separately.

MTAC reduces MAE relative to CEVAE, TEDVAE, and BSM-UR by 10.32%, 32.76%, and 34.61% on parking violations; 12.06%, 13.21%, and 21.29% on abandoned properties; and 6.42%, 8.56% and 3.87% on unsanitary conditions. The comparison on MSE is also consistent. This result demonstrates that MTAC learns a more accurate model because the task-agnostic mechanism is learned using data from multiple tasks. This jointly learned mechanism benefits the reconstruction of all three tasks. On the other hand, PLE does not model the causal relationship in report generation and only learns the association. On each dataset, MTAC reduces MAE by 13.07%, 5.58%, and 6.66% compared to PLE, respectively. And MTAC also outperforms PLE in MSE. This highlights the importance of modeling the causal relationship to avoid spurious associations. Besides, compare the MSE of MTAC with CEVAE, TEDVAE and BSM-UR on the abandoned property dataset, we find that the improvement is more significant than the other two datasets. This is because

Parking Violation		
Model	MAE	MSE
Multi-task	<b>0.2901</b>	<b>0.1634</b>
Single-task	0.3815	0.1833
Abandoned Property		
Model	MAE	MSE
Multi-task	<b>0.4280</b>	<b>0.1901</b>
Single-task	0.5042	0.2623
Unsanitary Condition		
Model	MAE	MSE
Multi-task	<b>0.3828</b>	<b>0.2496</b>
Single-task	0.3985	0.2635

**Table 3: Performance comparison for MTAC between multi-task training and single-task training.**

the abandoned property dataset is smaller than the other two. The task-shared mechanism cannot be trained sufficiently with only the abandoned property dataset.

#### 6.4 Multi-task v.s. Single-task

To further validate whether jointly learning the shared mechanism contributes to cause estimation, we train and test MTAC on each task separately. The comparison to jointly-trained MTAC is presented in Table 3. When jointly trained on all datasets, the prediction error of MTAC decreases compared to the model trained on each task separately. MAE and MSE decreased across all tasks: parking violation (0.0914, 0.0199), abandoned property (0.0762, 0.0722), and unsanitary condition (0.0978, 0.0139). This reduced prediction error in all three tasks demonstrates that jointly learning the task-agnostic causal mechanisms leads to a more accurate model. Particularly, the MSE on abandoned property has improved significantly due to joint-training. Again, this is because the size of the abandoned property dataset is small, and the SEMs of mechanism variables cannot be trained effectively using the single-task model. Therefore, joint-training significantly improves the mechanism variables' ability to represent  $p(W|Z)$  and further enhances urban event reconstruction performance.

#### 6.5 Causal Mechanism Validation Across Tasks

To demonstrate that the causal effects of the SES on reporting preferences are invariant across urban event types, we also evaluated the reconstruction performance by transferring the model parameters to an unseen task. We conduct a three-fold evaluation. In each fold, we select two tasks and train an MTAC as a teacher model, while a student model is trained on the remaining task. The shared backbone  $\theta^W$  is transferred from the teacher model to the student model using several transfer learning paradigms:

**Zero-shot:** For all mechanism variables, we replace the student model's shared backbone  $\theta^W$  in the SEMs with that of the teacher model. Then, the student model is evaluated directly without further fine-tuning.

**Head-only fine-tuning:** Starting from the same teacher initialization, we transfer the parameters of  $\theta^W$  to the student model and freeze this shared module. We then train only the target-task-specific parameters (i.e., the task-specific head  $\phi_{i,k}^W$  in SEMs for mechanism variables and SEMs for other variables) using the target-task training dataset while keeping the  $\theta^W$  fixed.

Trained on UC+PV, transferred to AP		
Model	MAE	MSE
Full fine-tuned	0.4753	0.2477
Head-only fine-tuned	<b>0.4696</b>	<b>0.2223</b>
Zero-shot	0.5912	0.3464
Single-task trained	0.5042	0.2623
Trained on UC+AP, transferred to PV		
Model	MAE	MSE
Full fine-tuned	<b>0.3523</b>	<b>0.1783</b>
Head-only fine-tuned	0.3800	0.1797
Zero-shot	0.4413	0.2236
Single-task trained	0.3815	0.1833
Trained on PV+AP, transferred to UC		
Model	MAE	MSE
Full fine-tuned	0.3933	<b>0.2512</b>
Head-only fine-tuned	<b>0.3910</b>	0.2541
Zero-shot	0.4301	0.2759
Single-task trained	0.3985	0.2635

**Table 4: Prediction Error of transferred MTAC. The transferred models are trained on two tasks and transferred to the other task. PV: parking violation; AP: abandoned property; UC: unsanitary condition.**

**Full fine-tuning:** For the fully fine-tuned student model,  $\theta^W$  is also optimized after being transferred from the teacher model.

Table 4 presents the prediction error of each student model on each dataset. The performance of a single-task trained version of MTAC is also included as a baseline. In all three evaluations, both the head-only and fully fine-tuned student models outperform the single-task trained model. Particularly, the head-only fine-tuned model uses the exact backbone  $\theta^W$  learned from the other two tasks. It shows higher accuracy than the single-task trained model in all three folds. This validates that the causal effect from the confounders to the mechanism variables holds invariance across tasks. When transferring to the abandoned property task, the reduction in both MAE and MSE is most significant compared to the other tasks. Again, this is due to the limited size of the abandoned property dataset. Moreover, the zero-shot model performs poorly on all tasks due to heterogeneity across tasks. The full fine-tuned model and head-only fine-tuned model perform similarly in each fold. This is because the task-shared backbone captures the task-agnostic patterns and is updated only slightly during full fine-tuning. The average normalized  $L_2$  distance between the task-shared backbone in fully fine-tuned and head-only fine-tuned model is 0.064, which represents a small parameter distance.

#### 6.6 Ablation Study

To understand the contribution of each component of MTAC, we conduct an ablation study. The results are presented in Table 5.

As inspired by [17, 26], there are 5 psychological paths that affect residents' reporting behavior. MTAC is set up with 5 mechanism variables accordingly for evaluation. When there are fewer mechanism variables, the prediction error increases for all three tasks. The result is demonstrated as  $|W| = 3$  and  $|W| = 1$  rows in Table 5. For the parking, abandoned property, and unsanitary condition datasets, MAE increased by 29.96%, 6.21%, and 0.37% with three mechanism variables, and by 34.78%, 10.68%, and 4.62% with one, respectively. The degradation in reconstruction loss with fewer mechanism variables indicates that the reporting preference

Model	Parking Violation		Abandoned Property		Unsanitary Condition	
	MAE	MSE	MAE	MSE	MAE	MSE
Complete MTAC	<b>0.2901</b>	<b>0.1634</b>	<b>0.4280</b>	<b>0.1901</b>	<b>0.3828</b>	<b>0.2496</b>
W  = 3	0.3770	0.1787	0.4546	0.2126	0.3842	0.2523
W  = 1	0.3910	0.1947	0.4737	0.2270	0.4005	0.2853
w/o MAP	0.5929	0.7390	1.5172	5.1866	0.5426	0.7221

**Table 5: Ablation study.**  $|W| = i$  represents MTAC model with  $i$  mechanism variables; For w/o MAP, MTCA that estimate the cause directly with the forward causal model without MAP.

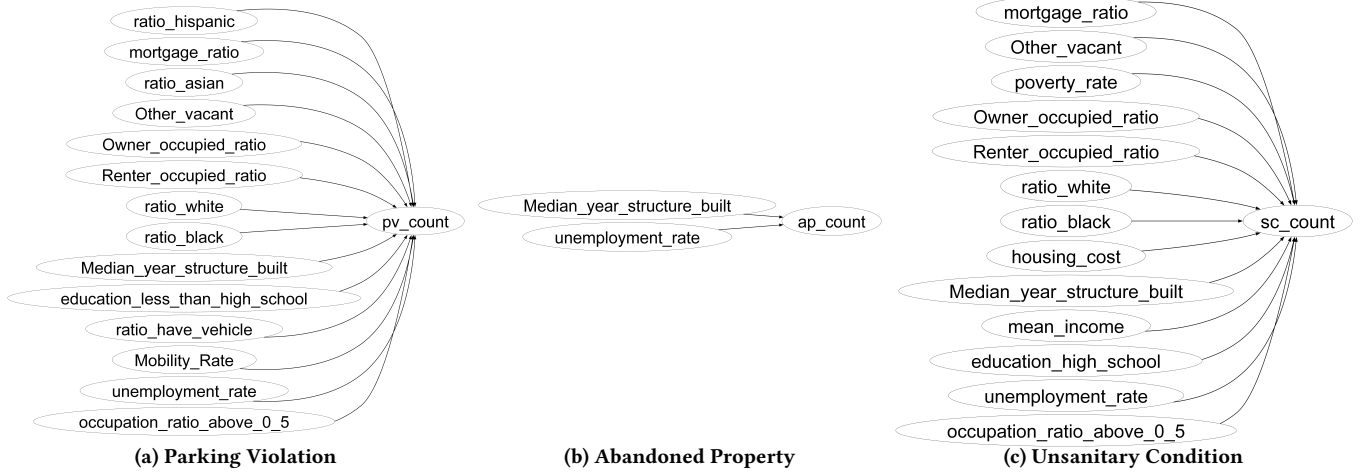


**Figure 5: Subgraph of the learned causal graph representing the generative mechanism of urban events.**

is high-dimensional. It is a compound effect of multiple psychological paths. As such, it is necessary for MTAC to have multiple mechanism variables to model reporting preferences. This result validates the multi-dimensional psychological path of residents' reporting behavior in [11, 17, 24, 26]

We also evaluate MTAC when the cause is estimated directly from the forward causal model instead of using the MAP-based inference algorithm. The prediction error increases significantly on all three tasks. On the abandoned property dataset, the MAE increases by 254.49%. This is because the causal model is a forward model, which computes the distribution of variables given its parental variables. Direct cause estimation only uses the SES information of residents but not the reports, i.e.,  $p(X|Z)$  rather than  $p(X|Z, Y)$ . Therefore, the direct estimation is highly inaccurate without the strongest indicator  $Y$ .

## 6.7 Causal Discovery

MTAC has learned the causal relationships between the confounders, the cause, and the outcome. These learned causal relationships provide explainability to the model, which is helpful for understanding the problem and explaining the cause estimation result. In the urban event reconstruction problem, it reveals which SES factors affect the occurrence of each type of urban event and the residents' reporting preferences. Figure 5 presents subgraphs of the learned causal graph, which illustrate the causal effect of residents' SES on urban event occurrence. The frequency of parking violation events is affected by resident's financial status (mortgage ratio and unemployment rate), race and culture (ratio of Hispanic, ratio of Asian, ratio of White people, and ratio of black people), educational attainment (ratio of people with less than a high school degree),

and the social environment that indicates the characteristic of the community (ratio of house renters/owners, median year built, mobility rate). Specifically, the ratio of families that own vehicles in the region plays an important role in the frequency of parking violations since it directly affects the demand for parking lots in the neighborhood. For the abandoned property problem, the financial status of residents and the housing conditions are significant causes. The occurrence of unsanitary issues is affected by the residents' financial status, race and culture, and educational attainment, as well as the social environment in the neighborhood. These generation mechanisms of urban events are consistent to the analysis in social studies [3, 21].

## 7 Conclusion

This work formulates the multi-task anti-causal learning problem and proposes MTAC to leverage the task-invariant causal effect for enhancing cause estimation. MTAC consists of a multi-task structural equation model while explicitly models the task-shared and task-specific causal effects on latent mechanism variables. The task-shared and task-specific mechanisms are explicitly captured using separate neural networks. An MAP-based inference algorithm is applied to invert the learned forward SEM for estimating the magnitude of causes from outcomes. Three urban event reconstruction tasks are evaluated as applications: parking violations, abandoned properties, and unsanitary conditions. Evaluation results show that jointly learning the shared mechanism improves reconstruction accuracy compared with single-task training, with particularly significant gains on the tasks with smaller datasets. The results also validate the shared causal mechanism across tasks.

## References

- [1] Gabriel Agostini, Emma Pierson, and Nikhil Garg. 2024. A Bayesian spatial model to correct under-reporting in urban crowdsourcing. In *Proceedings of the Thirty-Eighth AAAI Conference on Artificial Intelligence and Thirty-Sixth Conference on Innovative Applications of Artificial Intelligence and Fourteenth Symposium on Educational Advances in Artificial Intelligence (AAAI'24/IAAI'24/EAAI'24)*. AAAI Press, Article 2442, 9 pages. doi:10.1609/aaai.v38i20.30190
- [2] Md Manjurul Ahsan, Shahana Akter Luna, and Zahed Siddique. 2022. Machine-Learning-Based Disease Diagnosis: A Comprehensive Review. *Healthcare* 10, 3 (2022), 541. doi:10.3390/healthcare10030541
- [3] Noli Brazil, Brittany Vang, and Huda Abdelmur. 2024. Neighborhood inequality in government fines: The case of parking tickets in 16 U.S. cities. *Cities* 152 (2024), 105229. doi:10.1016/j.cities.2024.105229
- [4] Umair Muneer Butt, Sukumar Letchmunan, Mubashir Ali, and Hafiz Husnain Raza Sherazi. 2025. START: A Spatiotemporal Autoregressive Transformer for Enhancing Crime Prediction Accuracy. *IEEE Transactions on Computational Social Systems* 12, 6 (2025), 4650–4664. doi:10.1109/TCSS.2025.3550196
- [5] Umair Muneer Butt, Sukumar Letchmunan, Mubashir Ali, and Hafiz Husnain Raza Sherazi. 2025. START: A Spatiotemporal Autoregressive Transformer for Enhancing Crime Prediction Accuracy. *IEEE Transactions on Computational Social Systems* 12, 6 (2025), 4650–4664. doi:10.1109/TCSS.2025.3550196
- [6] Rich Caruana. 1997. Multitask Learning. *Machine Learning* 28, 1 (July 1997), 41–75. doi:10.1023/A:1007379606734
- [7] City of New York. 2024. OATH Hearings Division Case Status. NYC Open Data. [https://data.cityofnewyork.us/City-Government/OATH-Hearings-Division-Case-Status/jz4z-kudi/about\\_data](https://data.cityofnewyork.us/City-Government/OATH-Hearings-Division-Case-Status/jz4z-kudi/about_data)
- [8] City of New York. 2024. Parking Violations Issued - Fiscal Year 2024. NYC Open Data. <https://data.cityofnewyork.us/City-Government/Parking-Violations-Issued-Fiscal-Year-2024/pvqr-7yc4>
- [9] Scott Cook, Samantha Zuhlke, and Robin Saywitz. 2024. Potholes, 311 reports, and a theory of heterogeneous resident demand for city services. *Policy Studies Journal* 52 (06 2024), 647–669. doi:10.1111/psj.12540
- [10] Biwei Huang, Kun Zhang, Mingming Gong, and Clark Glymour. 2020. Causal Discovery from Multiple Data Sets with Non-Identical Variable Sets. *Proceedings of the AAAI Conference on Artificial Intelligence* 34, 06 (Apr. 2020), 10153–10161. doi:10.1609/aaai.v34i06.6575
- [11] Constantine Kontokosta, Boyeong Hong, and Kristi Korsberg. 2017. Equity in 311 reporting: Understanding socio-spatial differentials in the propensity to complain. *arXiv preprint arXiv:1710.02452* (2017).
- [12] Constantine E. Kontokosta and Boyeong Hong. 2021. Bias in smart city governance: How socio-spatial disparities in 311 complaint behavior impact the fairness of data-driven decisions. *Sustainable Cities and Society* 64 (2021), 102503. doi:10.1016/j.scs.2020.102503
- [13] Christos Louizos, Uri Shalit, Joris Mooij, David Sontag, Richard Zemel, and Max Welling. 2017. Causal effect inference with deep latent-variable models. In *Proceedings of the 31st International Conference on Neural Information Processing Systems* (Long Beach, California, USA) (NIPS'17). Curran Associates Inc., Red Hook, NY, USA, 6449–6459.
- [14] Dongming Luan, En Wang, Nan Jiang, Bo Yang, Yongjian Yang, and Jie Wu. 2024. A Data-Driven Crowdsensing Framework for Parking Violation Detection. *IEEE Transactions on Mobile Computing* 23, 6 (2024), 6921–6935. doi:10.1109/TMC.2023.3331429
- [15] Dongming Luan, En Wang, Nan Jiang, Bo Yang, Yongjian Yang, and Jie Wu. 2024. A Data-Driven Crowdsensing Framework for Parking Violation Detection. *IEEE Transactions on Mobile Computing* 23, 6 (2024), 6921–6935. doi:10.1109/TMC.2023.3331429
- [16] Gabriel Resende Machado, Eugênio Silva, and Ronaldo Ribeiro Goldschmidt. 2021. Adversarial Machine Learning in Image Classification: A Survey Towards the Defender's Perspective. *Comput. Surveys* 55, 1 (2021), Article 8. doi:10.1145/3485133
- [17] Terri Mannarini, Angela Fedi, and Stefania Trippetti. 2010. Public involvement: How to encourage citizen participation. *Journal of Community & Applied Social Psychology* 20, 4 (2010), 262–274. arXiv:https://onlinelibrary.wiley.com/doi/pdf/10.1002/casp.1030 doi:10.1002/casp.1030
- [18] Jianqiao Mao and Max A. Little. 2025. Mechanism Learning: reverse causal inference in the presence of multiple unknown confounding through causally weighted Gaussian mixture models. arXiv:2410.20057 [cs.LG] <https://arxiv.org/abs/2410.20057>
- [19] Scott McLachlan, Kudakwashe Dube, Graham A Hitman, Norman E Fenton, and Evangelia Kyrimi. 2020. Bayesian networks in healthcare: Distribution by medical condition. *Artificial Intelligence in Medicine* 107 (2020), 101912. doi:10.1016/j.artmed.2020.101912
- [20] Joris M. Mooij, Sara Magliacane, and Tom Claassen. 2020. Joint causal inference from multiple contexts. *J. Mach. Learn. Res.* 21, 1, Article 99 (Jan. 2020), 108 pages.
- [21] Victoria Chaney Morcel. 2013. Empty Neighborhoods: Using Constructs to Predict the Probability of Housing Abandonment. *Housing Policy Debate* 23, 3 (2013), 469–496. arXiv:https://doi.org/10.1080/10511482.2013.788051 doi:10.1080/10511482.2013.788051
- [22] NYC Open Data. [n. d.]. 311 Service Requests from 2020 to Present. NYC Open Data (Socrata dataset ID: erm2-nwe9). <https://data.cityofnewyork.us/Social-Services/311-Service-Requests-from-2020-to-Present/erm2-nwe9> Accessed: 2026-02-06.
- [23] Nick Pawłowski, Daniel C. Castro, and Ben Glocker. 2020. Deep structural causal models for tractable counterfactual inference. In *Proceedings of the 34th International Conference on Neural Information Processing Systems* (Vancouver, BC, Canada) (NIPS '20). Curran Associates Inc., Red Hook, NY, USA, Article 73, 13 pages.
- [24] N. Andrew Peterson and Robert J. Reid. 2003. Paths to psychological empowerment in an urban community: Sense of community and citizen participation in substance abuse prevention activities. *Journal of Community Psychology* 31, 1 (2003), 25–38. arXiv:https://onlinelibrary.wiley.com/doi/pdf/10.1002/jcop.10034 doi:10.1002/jcop.10034
- [25] Kristina Polotskaya, Carlos S. Muñoz-Valencia, Alejandro Rabasa, Jose A. Quesada-Rico, Domingo Orozco-Beltrán, and Xavier Barber. 2024. Bayesian Networks for the Diagnosis and Prognosis of Diseases: A Scoping Review. *Machine Learning and Knowledge Extraction* 6, 2 (2024), 1243–1262. doi:10.3390/make6020058
- [26] Dana Rotman, Jennifer Hammock, Jenny Preece, Derek Hansen, Carol Boston, Anne Bowser, and Yurong He. 2014. Motivations Affecting Initial and Long-Term Participation in Citizen Science Projects in Three Countries. (03 2014), doi:10.9776/14054
- [27] Bernhard Schölkopf, Dominik Janzing, Jonas Peters, Eleni Sgouritsa, Kun Zhang, and Joris Mooij. 2012. On causal and anticausal learning. In *Proceedings of the 29th International Conference on Neural Information Processing Systems* (Edinburgh, Scotland) (ICML '12). Omnipress, Madison, WI, USA, 459–466.
- [28] SeeClickFix. 2024. SeeClickFix - Newark, NJ. <https://seeclickfix.com/newark>
- [29] D. Srivastava, J. Xu, T. V. Vu, D. Liu, L. Li, P. Fu, S. Hou, N. Moreno Palmerola, Z. Shi, and R. M. Harrison. 2021. Insight into PM<sub>2.5</sub> sources by applying positive matrix factorization (PMF) at urban and rural sites of Beijing. *Atmospheric Chemistry and Physics* 21, 19 (2021), 14703–14724. doi:10.5194/acp-21-14703-2021
- [30] Hongyan Tang, Junjing Liu, Ming Zhao, and Xudong Gong. 2020. Progressive Layered Extraction (PLE): A Novel Multi-Task Learning (MTL) Model for Personalized Recommendations. In *Proceedings of the 14th ACM Conference on Recommender Systems* (Virtual Event, Brazil) (RecSys '20). Association for Computing Machinery, New York, NY, USA, 269–278. doi:10.1145/3383313.3412236
- [31] U.S. Census Bureau. [n. d.]. Explore Census Data (data.census.gov). Website. <https://data.census.gov/> Accessed: 2026-02-01.
- [32] Yilong Wang, Yuzhong Zhang, Xiangjun Tian, Xuhui Wang, Wenping Yuan, Jinzhi Ding, Fei Jiang, Zhe Jin, Weimin Ju, Ruosi Liang, Xiao Lu, Lu Shen, Shuai Sun, Tao Wang, Hongqin Zhang, Min Zhao, and Shilong Piao. 2025. Towards verifying and improving estimations of China's CO<sub>2</sub> and CH<sub>4</sub> budgets using atmospheric inversions. *National Science Review* 12, 4 (03 2025), nwaf090. arXiv:https://academic.oup.com/nsr/article-pdf/12/4/nwaf090/62350466/nwaf090.pdf doi:10.1093/nsr/nwaf090
- [33] Zepu Wang, Xiaobo Ma, Huajie Yang, Weimin Lyu, Yang Liu, Peng Sun, and Sharath Chandra Guntuku. 2025. Uncertainty-Aware Crime Prediction With Spatial Temporal Multivariate Graph Neural Networks. In *ICASSP 2025 - 2025 IEEE International Conference on Acoustics, Speech and Signal Processing (ICASSP)*. 1–5. doi:10.1109/ICASSP49660.2025.10889685
- [34] Zepu Wang, Xiaobo Ma, Huajie Yang, Weimin Lyu, Yang Liu, Peng Sun, and Sharath Chandra Guntuku. 2025. Uncertainty-Aware Crime Prediction With Spatial Temporal Multivariate Graph Neural Networks. In *ICASSP 2025 - 2025 IEEE International Conference on Acoustics, Speech and Signal Processing (ICASSP)*. 1–5. doi:10.1109/ICASSP49660.2025.10889685
- [35] Dezhi Yang, Guoxian Yu, Jun Wang, Jinglin Zhang, and Carlotta Domeniconi. 2025. Causal Discovery from Shifted Multiple Environments. In *Proceedings of the 31st ACM SIGKDD Conference on Knowledge Discovery and Data Mining V.1* (Toronto ON, Canada) (KDD '25). Association for Computing Machinery, New York, NY, USA, 1751–1762. doi:10.1145/3690624.3709247
- [36] Mingyang Zhang, Tong Li, Yue Yu, Yong Li, Pan Hui, and Yu Zheng. 2022. Urban Anomaly Analytics: Description, Detection, and Prediction. *IEEE Transactions on Big Data* 8, 3 (2022), 809–826. doi:10.1109/TBDDATA.2020.2991008
- [37] Weijia Zhang, Lin Liu, and Jiuyong Li. 2020. Treatment effect estimation with disentangled latent factors. In *AAAI Conference on Artificial Intelligence*. <https://api.semanticscholar.org/CorpusID:210943075>
- [38] Weijia Zhang, Lin Liu, and Jiuyong Li. 2021. Treatment Effect Estimation with Disentangled Latent Factors. *Proceedings of the AAAI Conference on Artificial Intelligence* 35, 12 (May 2021), 10923–10930. doi:10.1609/aaai.v35i12.17304
- [39] Xun Zheng, Bryon Aragam, Pradeep Ravikumar, and Eric P. Xing. 2018. DAGs with NO TEARS: continuous optimization for structure learning. In *Proceedings of the 32nd International Conference on Neural Information Processing Systems* (Montréal, Canada) (NIPS'18). Curran Associates Inc., Red Hook, NY, USA, 9492–9503.
- [40] Binbin Zhou, Hang Zhou, Weikun Wang, Liming Chen, Jianhua Ma, and Zengwei Zheng. 2024. HDM-GNN: A Heterogeneous Dynamic Multi-view Graph Neural

Network for Crime Prediction. *ACM Trans. Sen. Netw.* (May 2024). doi:10.1145/3665141 Just Accepted.

- [41] Binbin Zhou, Hang Zhou, Weikun Wang, Liming Chen, Jianhua Ma, and Zengwei Zheng. 2024. HDM-GNN: A Heterogeneous Dynamic Multi-view Graph Neural

Network for Crime Prediction. *ACM Trans. Sen. Netw.* (May 2024). doi:10.1145/3665141 Just Accepted.